

## Distinct degradation processes in ZnO varistors: reliability analysis and modeling with accelerated AC tests

Hadi YADAVARI, Mustafa ALTUN\*

Faculty of Electrical and Electronics Engineering, İstanbul Technical University, İstanbul, Turkey

Received: 13.06.2016

Accepted/Published Online: 30.12.2016

Final Version: 30.07.2017

**Abstract:** In this study, we investigate different degradation mechanisms of zinc oxide (ZnO) varistors. We propose a model that shows how  $V_v$  (defined as DC varistor voltage when a 1-mA DC current is applied) changes with time for different stress levels. For this purpose, accelerated degradation tests are applied for different AC current levels and voltage values are then measured. Different from the common practice in the literature that considers degradation with only decreasing  $V_v$  values, we demonstrate either an increasing or a decreasing trend in the  $V_v$  parameter. The tests show a decreasing trend in  $V_v$  for current levels above a certain threshold and an increasing trend for current levels below this threshold. Considering both of these degradation mechanisms, we present a mathematical degradation model. The proposed model exploits the physics of the degradations for a single-grain boundary that is the core structure of a ZnO varistor. To validate the proposed model, we perform Monte Carlo simulations and the results are compared with those obtained from accelerated AC tests. As a summary of this study, we introduce a conceptual accelerated AC test methodology to analyze the reliability of the new ZnO varistor.

**Key words:** Reliability analysis and modeling, degradation, ZnO varistors, AC tests

### 1. Introduction

Zinc oxide (ZnO) varistors have widely been used in electrical and electronics systems against overvoltage surges thanks to their nonohmic current–voltage characteristics and excellent energy-handling capabilities [1–3]. ZnO varistors are variable resistors used for limiting or diverting transient AC line voltage; they are usually subjected to long-term AC voltage and surge stresses that lead to their degradation. Even varistors used within their well-defined specifications might fail due to degradation. An aging phenomenon degrades the varistors and thermally breaks them down or destroys them [4]. Therefore, a degradation analysis of varistors is crucial.

An overwhelming majority of the studies in the literature have reported increasing leakage current and accordingly an increasing  $V_v$  parameter (defined as DC varistor voltage when a 1-mA DC current is applied) that manifests the degradation [1,5–8]. However, the decreasing leakage current that results in an increase in  $V_v$  is totally disregarded. Only a few studies have mentioned this, but without detailed analysis [9,10]. The reason is that as opposed to an increasing leakage current, a decreasing leakage current might not be hazardous for a varistor. However, we show that this kind of degradation directly affects system reliability and safety [11]. This is illustrated in Figure 1. Even a slight increase in  $V_v$  can lead to a dramatic change in the maximum designed voltage criteria for other components in the same block, especially for those in the power supply block. This eventually causes a breakdown of protected circuits and components. This phenomenon is demonstrated

\*Correspondence: altunmus@itu.edu.tr

with the testing of over 100 electronic cards that were commercially used but subsequently failed due to varistor degradation [11]. As a result, to our knowledge, this is the first study on the modeling and characterization of ZnO varistors regarding both degradation processes.

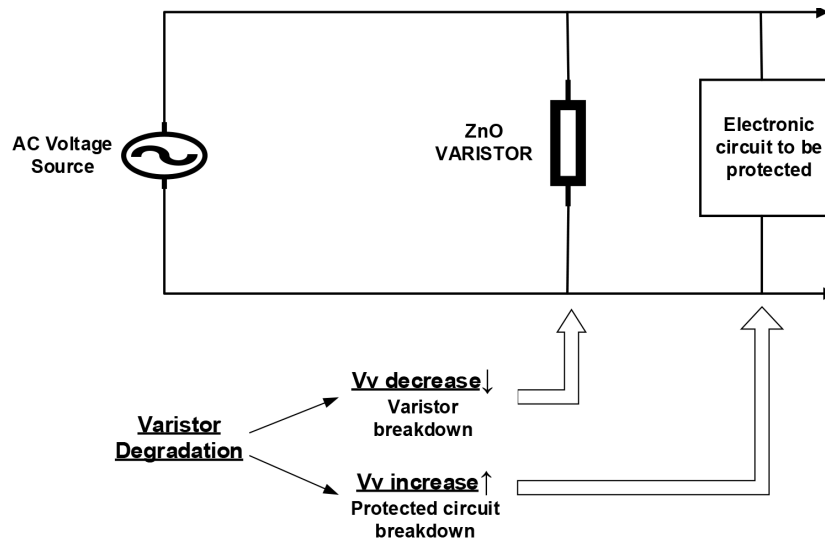


**Figure 1.** Breakdown of the system in the case of different degradation processes of the ZnO varistor [11].

We perform accelerated AC voltage/current tests to analyze varistor degradation. In general, accelerated tests are conducted by applying stresses such as temperature, vibration, humidity, and voltage beyond their normal expected levels in the field [12,13]. We use the single stress variable of voltage since it is by far the most dominant stress type for varistors. There are two major reliability/degradation test methodologies for varistors: pulse tests (8/20- $\mu$ s and 2-ms tests) and accelerated AC tests. We use accelerated AC tests since they are cost-efficient both in terms of test time and test equipment.

In the literature, there are studies that use AC tests by showing that the  $V_v$  parameter of varistors, which is one of the key parameters related to measuring the reliability of a varistor, can be changed during the tests [7,11,14]. In this study, we focus on the reasoning, justification, and modeling of these  $V_v$  changes. By applying accelerated AC signals, we see either an increasing or a decreasing trend in  $V_v$  that depends on the current levels passing through the varistor. The tests show a continuous and rapidly decreasing trend in  $V_v$  for current levels above a certain threshold and a slow increasing trend for current levels below the threshold. Although we apply accelerated AC tests to a particular metal-oxide varistor (detailed information such as the composition, microstructure, and phases of this particular ZnO varistor is available in [15]), our results are generally applicable to a variety of similar metal-oxide varistors.

We investigate the physical bases of the degradation processes observed in the AC tests. Physically, a ZnO varistor contains numerous pieces of zinc oxide grains of different shape and sizes, along with other metal oxide additives [15]. Several studies demonstrated that electrical stresses on varistors cause a deformation of their highly resistive grain boundary potential barriers [5,16,17]. It has also been reported that mild degradation after applying an electric field stress leads to a decrease in the effective doping concentration of the grains and accordingly to an increase in the resistance of grain boundaries [6]. However, applying a strong electrical field might lead to an increase in the doping concentration, resulting in a decrease in the resistance of grain boundaries [18]. Motivated by this, in our model, we assume that every single ZnO–ZnO grain boundary can be

considered as a resistor. We formulate the resistor as a function of time and applied stress that determines the relative effects of the degradation processes. We need to additionally determine how to combine the resistors by considering grain shapes and grain amounts. In this regard, several studies have been proposed on varistor microstructures that considered grain shape and topology, as well as type and distribution of defects [19–21]. In a similar way, we present a simple yet accurate microstructure that solely consists of grain boundary resistors. We perform a Monte Carlo method to validate our model; the outcomes of the simulations match well with the results obtained from the accelerated AC degradation tests.

The outline of paper is as follows. In Section 2, the proposed accelerated AC test methodology used to distinguish degradation processes is presented. In Section 3, the physical bases of the processes are presented and used to form a varistor degradation model. Simulation results are also given to validate the proposed model. In Section 4, a reliability test methodology is presented to facilitate and summarize the steps proposed in this study. Section 5 outlines the conclusion of this work.

## 2. Degradation processes by accelerated AC tests

In order to investigate varistor degradation mechanisms, we perform accelerated AC tests that are cost-efficient both in terms of test time and test equipment. The tests show different degradation processes including stable, decreasing, and increasing trends in  $V_v$ , depending on the applied AC signal levels. Different accelerated AC signal levels are applied on varistor samples with a diameter of 12 mm and a height of 15 mm, as shown in Figure 2. We number the varistors from Var1 to Var11. The samples have the same material, manufacture, and characteristics [15].

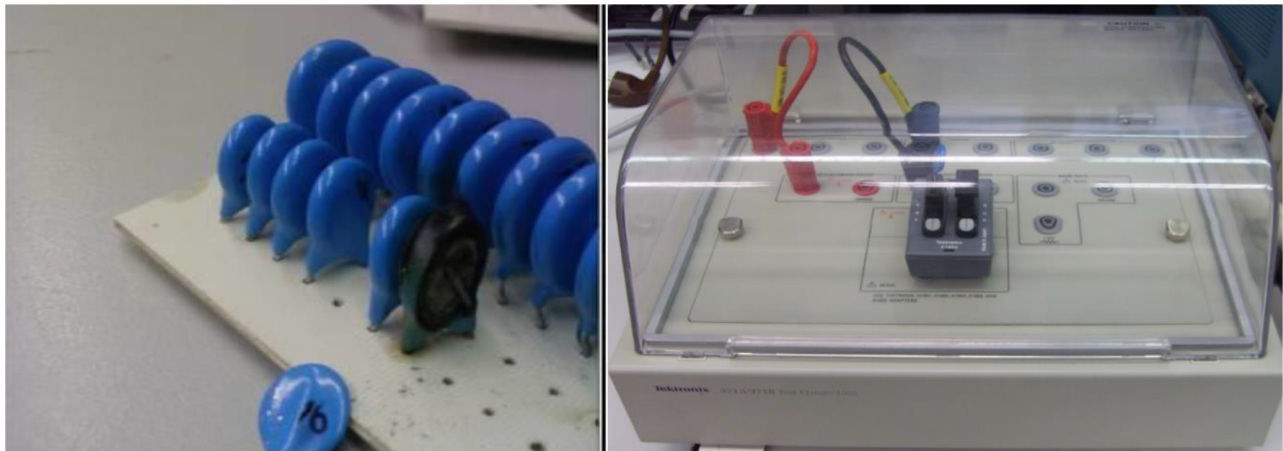


**Figure 2.** Varistor samples used in the accelerated AC tests.

For a specific AC current passing through a varistor called  $I_{VAR}$  (RMS value), voltage values of the varistor called  $V_{VAR}$  (RMS value) are periodically measured. Our three-step test procedure is summarized as follows:

1. All samples are shorted to ground for 24 h in order eliminate any previous capacitive/inductive loads.
2.  $I_{VAR}$  is determined and continuously applied.  $V_{VAR}$  values are then periodically measured in a 300-min time period. If the varistor burns, then the tests are stopped at the time of the breakdown (failure).

3. Step 2 is repeated for different  $I_{VAR}$  values to analyze different degradation mechanisms and finally to find the  $I_{VAR}$  threshold value.

For the second step, we need to determine which  $I_{VAR}$  values are used. The suggested  $I_{VAR}$  value according to IEC standard IEC-60099-4 is 1 mA [22]. However, we show that applying different  $I_{VAR}$  values results in different degradation mechanisms. This is illustrated in Figure 3 using six different  $I_{VAR}$  values: 5 mA, 3 mA, 2 mA, 1.5 mA, 1 mA, and 0.7 mA. Note that for each  $I_{VAR}$  value, multiple samples are generally used to take into account probable process variations. Analyzing the results in Figure 3, we clearly see two different degradation mechanisms corresponding to increasing and decreasing  $V_{VAR}$  values over time. While a decrease in  $V_{VAR}$  results in an increase in leakage current and a decrease in  $V_V$ , the increase in  $V_{VAR}$  makes the leakage current decrease and  $V_V$  increase. Note that a varistor voltage  $V_V$  represents a varistor voltage when a 1-mA DC current is conducted. Therefore, there is a positive correlation between  $V_{VAR}$  and  $V_V$  if a considerable amount of varistor current is conducted in the range of mA values. In the following section, we separately analyze the cases in Figure 3 to find the threshold value of  $I_{VAR}$  that distinguishes between degradation mechanisms.

## 2.1. Finding the threshold

In order to find the threshold value, we first tried  $I_{VAR} = 10$  mA. The varistor voltage plunged dramatically and, after several seconds, the varistor started to burn up. We decreased the value to 5 mA, but there was still a dramatic decline in varistor voltage. We then performed tests at  $I_{VAR} = 2$  mA for two samples, as shown in Figure 4a. We do not have not full data covering the entire 300 min since the varistors started to burn up. We continued reducing  $I_{VAR}$  until the  $V_{VAR}$  values stabilized with time. This was achieved when  $I_{VAR} = 1.5$  mA. As shown in Figure 4b, when  $I_{VAR} = 1.5$  mA,  $V_{VAR}$  shows a slight decrease. This means that the threshold value is slightly under 1.5 mA. We repeated the test for  $I_{VAR} = 1$  mA and  $I_{VAR} = 0.7$  mA, as shown in Figures 5a and 5b, respectively.

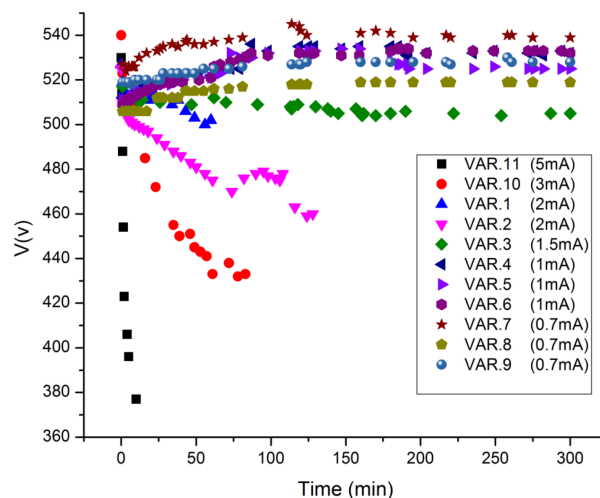


**Figure 3.** Accelerated degradation tests results;  $V_{VAR}$  values in the time domain for different  $V_{VAR}$  values.

In conclusion, for current levels above 1.5 mA, which was found to be the threshold value for this family of varistor samples,  $V_{VAR}$  drops dramatically until it burns up. We classify this as a hard degradation mechanism. On the other hand, for current levels below the threshold value (1.5 mA), we see a relatively slow increasing

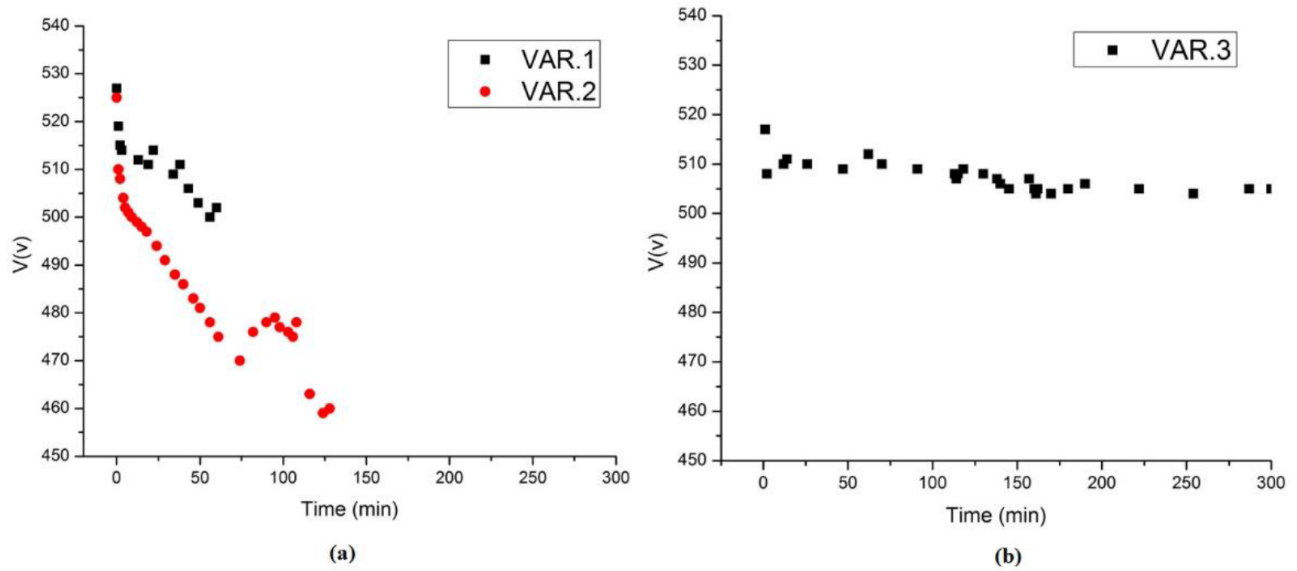


**Figure 4.** Accelerated degradation tests results:  $V_{VAR}$  values in the time domain for a)  $I_{VAR} = 2 \text{ mA}$  and b)  $I_{VAR} = 1.5 \text{ mA}$ .

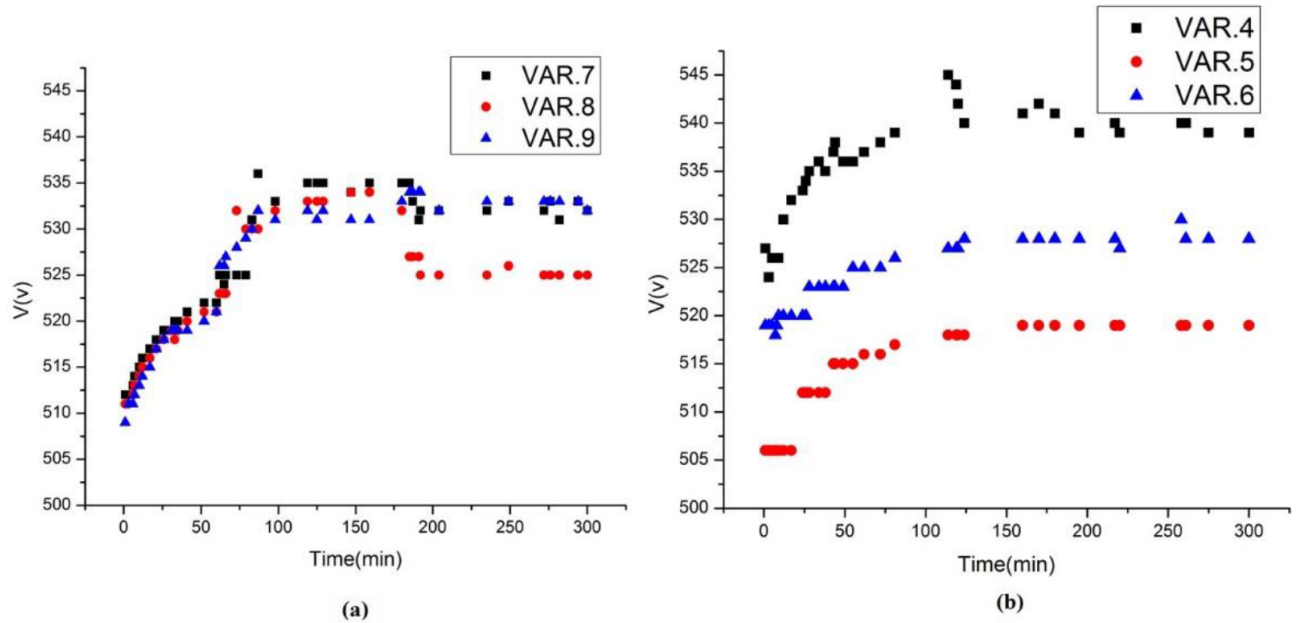


**Figure 5.** Accelerated degradation tests results:  $V_{VAR}$  values in the time domain for a)  $I_{VAR} = 1 \text{ mA}$  and b)  $I_{VAR} = 0.7 \text{ mA}$ .

trend in  $V_{VAR}$ . We classify this as a mild degradation mechanism.

### 3. Physical bases of degradation processes and mathematical modeling

In this section, we aim to develop a mathematical reliability model for varistor degradation. For this purpose, we first investigate the physical bases of the degradation processes observed in the AC tests. It is a general concept that electrical stresses on varistors cause deformation of grain boundary potential barriers [5,16,17]. Figure 6

shows a conceptual microstructure of a ZnO varistor, in which the grains and boundaries are represented by white and gray regions, respectively. If boundaries are surpassed, then a current is conducted through paths of grains illustrated by the arrows in the figure. Note that while ZnO grains are conductive, intergranular boundaries are highly resistive. Since ZnO grains and boundaries are spread in an almost regular fashion, a single grain boundary between two grains can be used as a core structure for varistor models. This is called a single-grain boundary model [23,24].

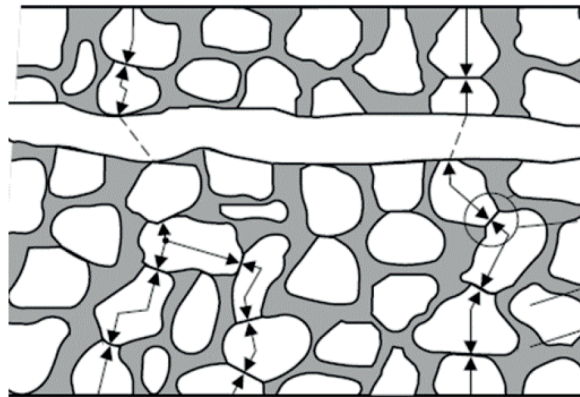


**Figure 6.** Microstructure of a varistor element [15].

A ZnO–ZnO grain boundary can be modeled with a Schottky barrier, as shown in Figure 7. With the depletion of carriers from surrounding grains, a double Schottky barrier forms. Long-term stresses cause degradation, along with a change in barrier height and characteristics due to the migration of ionized donors in the electric field and their redistribution in the near-surface region of the grains. This results in an increase in leakage current and, relevantly, a decrease in  $V_v$  [25].

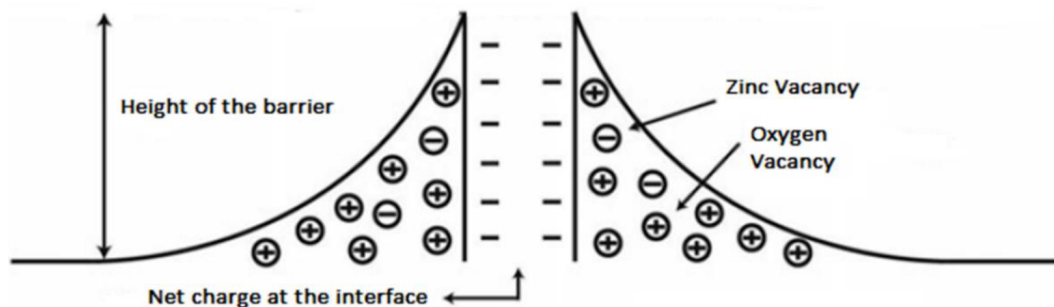


**Figure 7.** A simple double Schottky barrier model of a ZnO/ZnO grain boundary.

Other possible mechanisms of deformation of grain boundary barriers explain different processes of degradation in ZnO varistors. It has been reported that there are two types of electron traps of importance for ZnO varistors: traps located at the ZnO–ZnO grain boundaries, known as interface traps, and traps located within the bulk of ZnO grains, known as bulk traps. Interface trapping of electrons is generally considered to be the mechanism that gives rise to double Schottky barriers at grain boundaries [26].

Furthermore, it has been reported that mild degradation after applying an electric field stress leads to a decrease in the effective doping concentration at the grains and accordingly to an increase in the resistance of grain boundaries [6]. This increase clearly explains the increase in  $V_v$ . On the other hand, applying a strong

electrical field might lead to an increase in the doping concentration, resulting in a decrease in the resistance of grain boundaries [18]. Subsequently, it results in a decrease in Vv.

Motivated by the previously mentioned studies on the physics of degradation demonstrating the change in grain boundary resistance values for different stress types, we model every single-grain boundary barrier as a resistor. The resistor value can change according to applied stress in either an increasing or decreasing trend. In this study, we therefore contribute to a nonlinear cross-boundary resistor as a function of time and stress. This is illustrated in Figure 8.

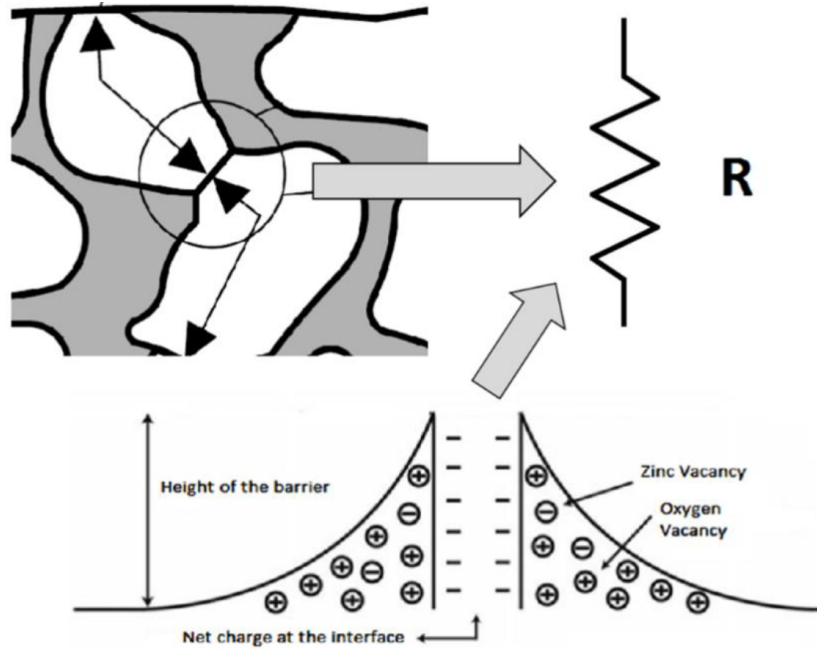


Figure 8. Modeling of a single grain boundary as a resistor.

The proposed model formula for a single resistor (grain boundary) is shown below:

$$R_i(t)sR_{in}(1 + \alpha R_i(t)R_i(s) \beta R_d(t)R_d(s)). \tag{1}$$

Degradation depends on both stress (s) and time (t). The initial value of the resistor, the degradation-free value, is represented by R, and this is obtained using initial  $V_{VAR}$  and  $I_{VAR}$  values. Degradation mechanisms causing an increase in Vv and a decrease in Vv in the time domain are represented by  $R_i(t)$  and  $R_d(t)$  functions, respectively. We select  $R_i(t) = \exp(-nt^{1/m})$  for AC signal stresses. We select  $R_d(t) = 1/\sqrt{t}$ , which is derived using the leakage current formula given in [16]. Although there is a common consensus in the literature for decreasing Vv behavior in the time domain shown by  $R_d(t)$ , the increasing Vv behavior and corresponding physical models lack precision. Therefore, in the determination of  $R_i(t)$ , our main source is the test data obtained from our experiments. The functions  $R_i(s)$  and  $R_d(s)$  represent the effects of applied stresses on degradation. They could be in the form of the following exponential/power functions [27]:

- Arrhenius  $R(s) = e^{c/s}$
- Eyring  $R(s) = s^{-1} e^{c/s}$
- Inverse power law  $R(s) = s^n$

Note that since the above equations are used for a single stress ( $s$ ), they can be applicable in our case using  $s = I_{VAR}$ . In our accelerated tests, we use a single stress of current  $I_{VAR}$ . According to the tests described in Section 2, the threshold current ( $I_{VAR-th}$ ) is close to 1.5 mA, determining the effects and dominance of  $R_i(s)$  and  $R_d(s)$  for different  $I_{VAR}$  levels. Observing this, we select  $R_i(s) = (1 - e^{-cs})$  and  $R_d(s) = e^{c(s-I_{VAR-th})}$ , where  $s = I_{VAR}$ . The coefficients in the degradation formula  $\alpha$ ,  $\beta$ ,  $n$ ,  $m$ , and  $c$  are empirically calculated using the test data. As a result,  $\alpha = 0.003$ ,  $\beta = 0.001$ ,  $n = 0.1$ ,  $m = 0.7$ , and  $c = 4000$ .

### 3.1. Varistor microstructure formation and simulation results

Varistor ceramics are compounds from ZnO grains of different shapes, sizes, and orientations. Since ZnO grains have predictable sizes, the total number of grains in a varistor can be found by using the varistor size [15]. Suppose that each grain diameter is in the range between 10  $\mu\text{m}$  and 100  $\mu\text{m}$ , and a ZnO varistor has a size of nearly 5 mm  $\times$  10 mm in two dimensions [15] (the test samples) that results in 5000 to 0.5 million grains. Using these relatively high numbers of grains or grain boundaries and corresponding nonlinear resistors in simulations is certainly impractical, so we need a microstructure. Figure 9 shows a simplified varistor microstructure based on equal cubic grains or square grains on a mesh that represents all grains and boundaries [19,20]. We exploit this structure by using resistors only for grain boundaries.

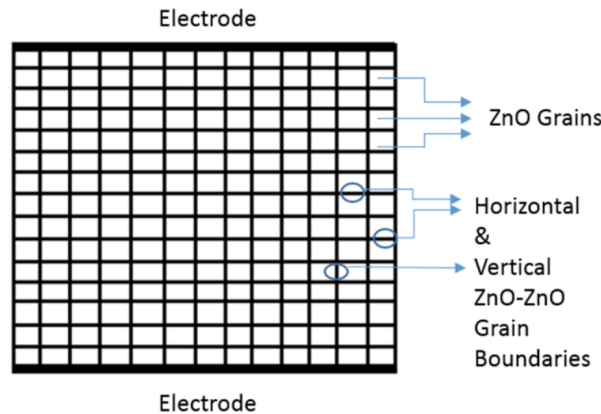


Figure 9. Simplified grain model of a varistor.

Considering the tested varistor dimensions, we use  $X$  and  $3X$  number of vertical and horizontal squares, respectively. Increasing the value of  $X$  here results in better accuracy at the cost of poor runtime and complexity for the simulation. Therefore, we need to determine the minimum value of  $X$  for which we can achieve relatively high accuracy. In order to do this, we start with  $X = 1$  and increase  $X$  one by one. It is apparent that for  $X = 1$ , there is no vertical grain boundary. For  $X = 2$  and  $X = 3$ , the corresponding microstructures are shown in Figure 10. For each case, we perform a Monte Carlo analysis using multiple samples. This is illustrated in Figure 11. For all four graphs in the figure, we use test data obtained using  $I_{VAR} = 2$  mA. According to Figure 11, as expected, increasing  $X$  or the number of resistors improves the simulation accuracy that depends on the fluctuations between samples as well as the curve fitness to the test data. Analyzing the results in the figure, we conclude that cases  $X = 3$  (26 resistors) and  $X = 4$  (58 resistors) have similar performances. Trying larger  $X$  values also produces very similar results. Therefore, we use  $X = 3$  with 58 resistors in further simulations.

Figure 12 shows the results comparing the test data obtained using  $I_{VAR}$ s of 0.7 mA, 1 mA, 1.5 mA, and 2 mA and the related curves obtained using the proposed microstructure with 58 resistors. Note that since

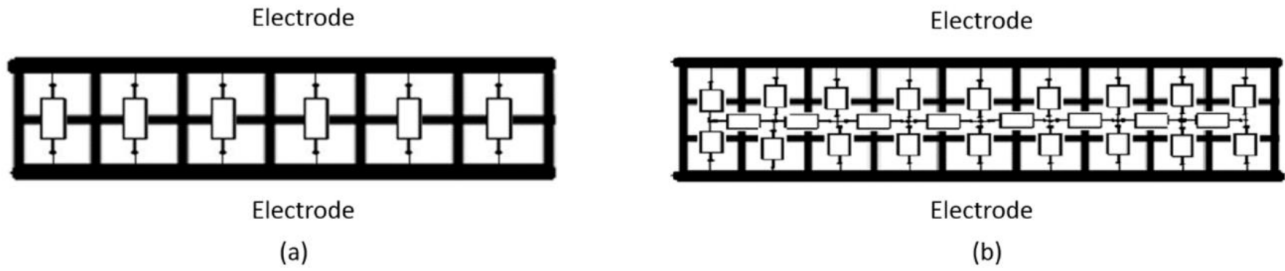


Figure 10. Proposed microstructures a)  $X = 2$ , 6 resistors and b)  $X = 3$ , 26 resistors.

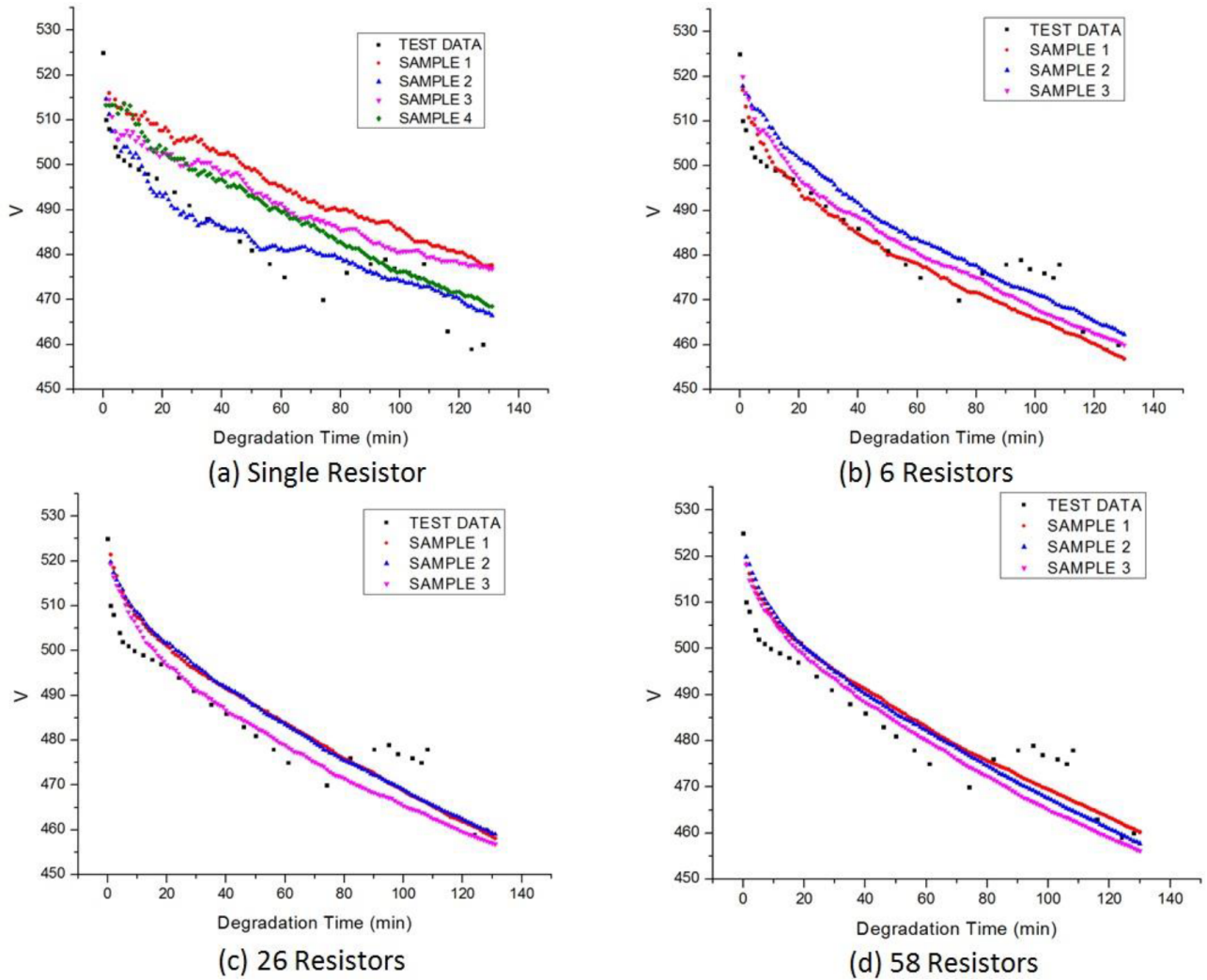
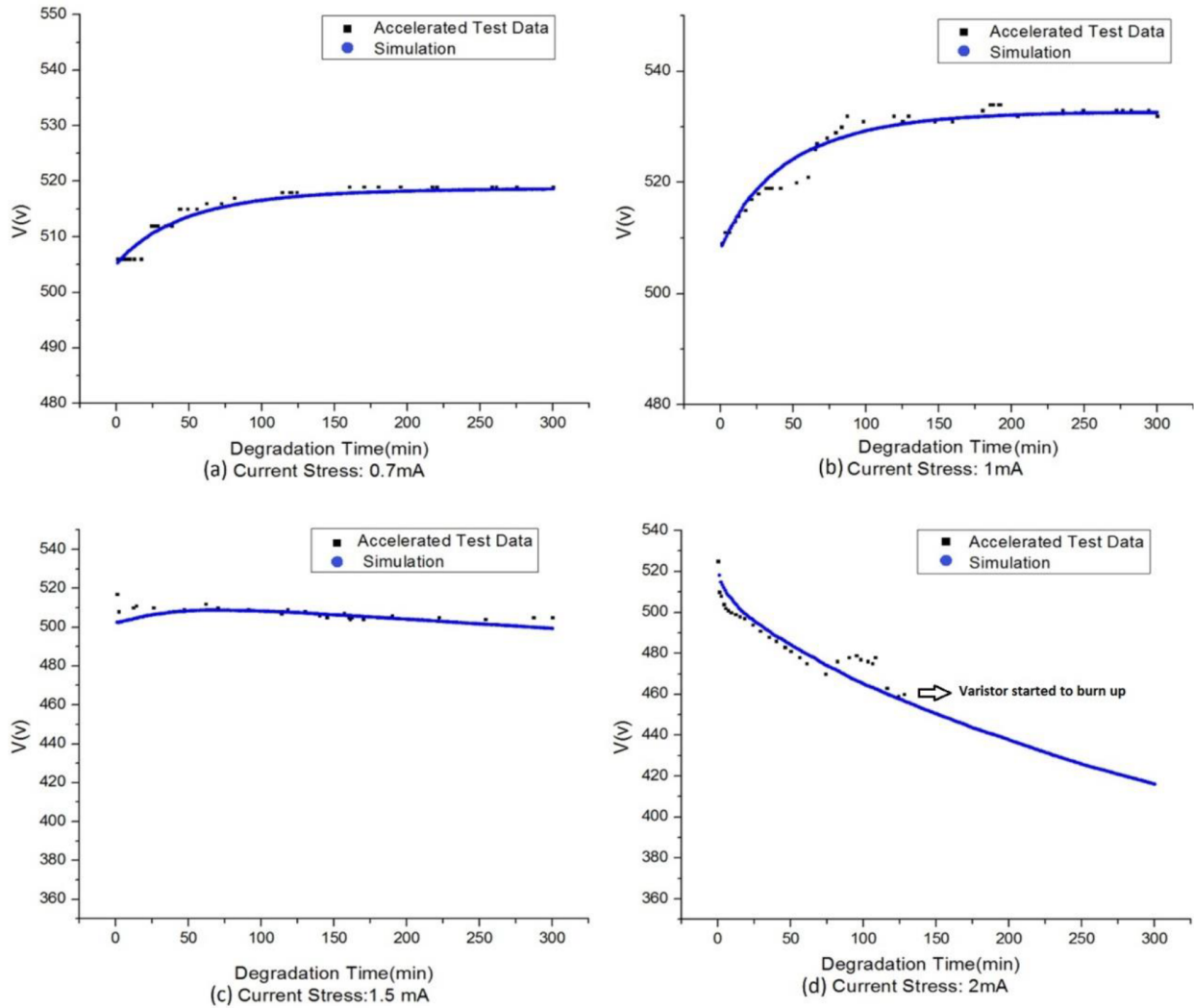


Figure 11. Simulation results in comparison with the AC test data for a) single resistor, b)  $X = 2$ , 6 resistors, c)  $X = 3$ , 26 resistors, and d)  $X = 4$ , 58 resistors.

the varistor started to burn up after 130 min at a stress level of 2 mA of current, there are limited test data for this stress level. Each of the 58 resistors is independently treated using Eq. (1). The results clearly prove the accuracy of the proposed model; there is almost a perfect match between the curves and the real test points.



**Figure 12.** Accelerated degradation test data compared to the simulation results for a)  $I_{VAR} = 0.7$  mA, b)  $I_{VAR} = 1$  mA, c)  $I_{VAR} = 1.5$  mA, and d)  $I_{VAR} = 2$  mA current stresses.

#### 4. Reliability test methodology for a new varistor

A variety of endurance and environmental tests are conducted to assure the reliability of ZnO varistors. These tests derived from the extremes of expected application conditions, with test conditions intensified to obtain authoritative results within a reasonable period [14]. The most commonly used test methodologies include surge current derating ( $8/20 \mu s$ ), surge current derating (2 ms), fast temperature cycling, and vibration tests. These test methodologies are usually costly in terms of test time and test equipment. Additionally, only FAIL/PASS criteria are considered for most of these methodologies, so they lack the analyzing reliability performance of varistors in the time domain. They also neglect the different varistor degradation mechanisms explained thoroughly in the previous sections. Considering these drawbacks, we present a simple yet efficient test methodology to assess the reliability of a ZnO varistor based on accelerated AC degradation tests. Figure 13 shows a flowchart of the proposed methodology. According to the flowchart, it is possible to analyze varistor reliability based on accelerated degradation AC tests by using the proposed degradation model.

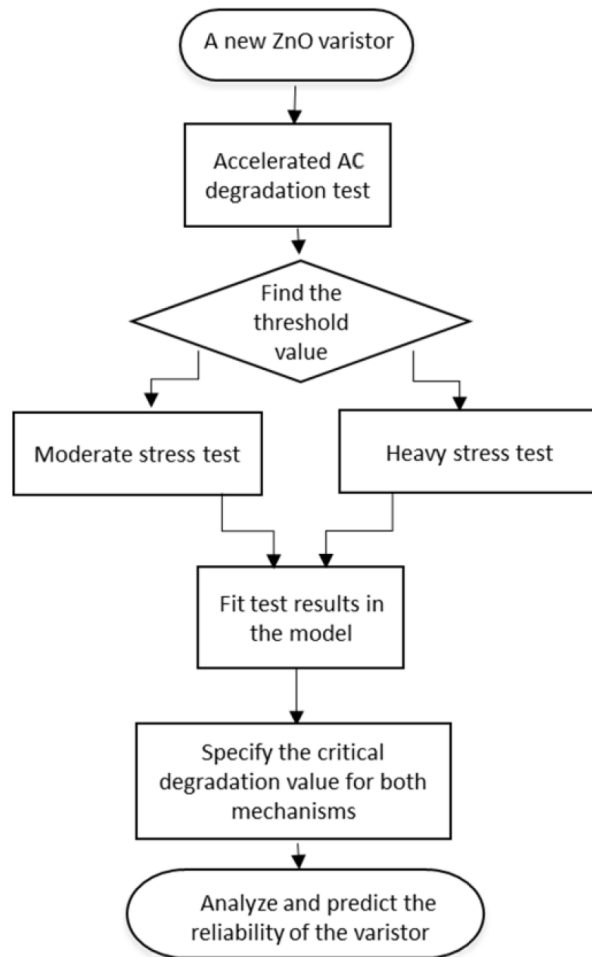


**Figure 13.** Reliability test methodology flowchart for ZnO varistors.

First, accelerated AC tests are applied to find the threshold value that distinguishes between the degradation mechanisms. As examined in Section 2, the threshold value of ZnO varistors should be close to a 1-mA current. Second, both heavy and moderate degradation tests are performed to specify the trend of the mechanisms. Third, the proposed degradation model is used. The test data are fitted to the model by calculating the empirical coefficients from the experiments. By considering the obtained degradation formula and the tested varistor usage in a field, different critical degradation values can be chosen by designers. Finally, varistor reliability can be estimated. Note that the proposed methodology is conceptually given without certain procedures and steps having specific numbers for different varistor families. These details are outside of the scope of this study and can be considered in future work.

## 5. Conclusion

In this paper, we study degradation processes for ZnO varistors. For this purpose, accelerated AC degradation tests are applied aiming to measure varistor voltage values in the time domain. Different from the common practice in the literature that considers degradation with decreasing  $V_v$  values only, the tests show either an increasing or a decreasing trend in the  $V_v$  parameter. To justify the observed degradation processes, the physical bases of the degradations are investigated. To do this, a single grain boundary (Schottky barrier) is modeled as a

nonlinear resistor. Its characteristics in the time domain change with the applied stress levels. A microstructure is then formed using these boundary resistors.

We perform a Monte Carlo method to validate the proposed varistor degradation model, and the outcomes of the simulations match well with the results obtained from the accelerated AC degradation tests. To summarize, we introduce a conceptual accelerated AC test methodology to conduct a reliability analysis of a new ZnO varistor.

### Acknowledgments

This work was done in cooperation with Arçelik A.Ş. and supported by the TÜBİTAK (Scientific and Technological Research Council of Turkey) University–Industry Collaboration Grant Program #5130034. We are grateful to Burak Şal from İstanbul Technical University for his help with the experiments and Ahmet Ferit Coşan and Bariş Ocak from Arçelik A.Ş. for their feedback and discussions.

### References

- [1] Clarke DR. Varistor ceramics. *J Am Ceram Soc* 1999; 82: 485-502.
- [2] Mahmud S, Johar AM, Putrus GA, Chong J, Karim MA. Nanostructure of ZnO fabricated via French process and its correlation to electrical properties of semiconducting varistors. *Synth React Inorg Me* 2006; 36: 155-159.
- [3] Gupta TK. Application of zinc oxide varistors. *J Am Ceram Soc* 1990; 73: 1817-1840.
- [4] Brown K. Metal oxide varistor degradation. *IAEI Magazine*, March 2004. Available online at <http://iaeimagazine.org/magazine/2004/03/16/metal-oxide-varistor-degradation/>.
- [5] Eda K, Iga A, Matsuoka M. Degradation mechanism of non-Ohmic zinc oxide ceramics. *J Appl Phys* 1980; 51: 2678-2684.
- [6] Ponce MA, Macchi C, Schipani F, Aldao CM, Somoza A. Mild degradation processes in ZnO-based varistors: the role of Zn vacancies. *Philos Mag* 2015; 95: 730-743.
- [7] Tsukamoto N. Study of degradation by impulse having 4/10  $\mu$ s and 8/20  $\mu$ s waveform for MOVs (metal oxide varistors). In: *International Conference on Lighting Protection*; 2014. New York, NY, USA: IEEE. pp. 620-623.
- [8] Liu J, He J, Hu J, Long W, Luo F. Statistics on the AC ageing characteristics of single grain boundaries of ZnO varistor. *Mater Chem Phys* 2011; 125: 9-11.
- [9] Sato K, Takada Y, Takemura T, Ototake M. A mechanism of degradation in leakage currents through ZnO varistors. *J Appl Phys* 1982; 53: 8819-8826.
- [10] Zhao X, Li J, Li H, Li S. The impulse current degradation of ZnO varistor ceramics. In: *Proceedings of the International Conference on Electrical Insulating Materials*; 2011. New York, NY, USA: IEEE. pp. 43-46.
- [11] Yadavari H, Sal B, Altun M, Erturk EN, Ocak B. Effects of ZnO varistor degradation on the overvoltage protection mechanism of electronic boards. *Safety and Reliability of Complex Engineered Systems* 2015; 269: 2153-2160.
- [12] Nelson WB. *Accelerated Testing: Statistical Models, Test Plans, and Data Analysis*. New York, NY, USA: John Wiley & Sons; 2009.
- [13] Meeker WQ, Escobar LA. *Statistical Methods for Reliability Data*. New York, NY, USA: John Wiley & Sons; 2014.
- [14] Mardira KP, Saha TK, Sutton RA. The effects of electrical degradation on the microstructure of metal oxide varistor. In: *Transmission and Distribution Conference and Exposition*; 2001. New York, NY, USA: IEEE/PES. pp. 329-334.
- [15] Epcos AG. *Data Book for SIOV Metal Oxide Varistors*. Munich, Germany: Epcos AG; 2008.

- [16] Sato K, Takada Y, Takemura T, Ototake M. A mechanism of degradation in leakage currents through ZnO varistors. *J Appl Phys* 1982; 53: 8819-8826.
- [17] Hayashi M, Haba M, Hirano S, Okamoto M, Watanabe M. Degradation mechanism of zinc oxide varistors under dc bias. *J Appl Phys* 1982; 53: 5754-5762.
- [18] Ponce MA, Ramirez MA, Parra R, Malagu C, Castro MS, Bueno PR, Varela JA. Influence of degradation on the electrical conduction process in ZnO and SnO<sub>2</sub>-based varistors. *J Appl Phys* 2010; 108: 074505
- [19] Bavelis K, Gjonaj E, Weiland T. Modeling of electrical transport in zinc oxide varistors. *Advances in Radio Science* 2014; 12: 29-34.
- [20] Meshkatoddini MR. Statistical study of the thin metal-oxide varistor ceramics. *Australian Journal of Basic and Applied Sciences* 2010; 4: 751-763.
- [21] Wang L, Wu W, Li XG, Zhang Y. Two different micromodels of zinc oxide varistors. *J Appl Phys* 1995; 77: 5982-5986.
- [22] International Electrotechnical Commission. IEC 60099-4. Surge Arresters Part 4: Metal-Oxide Surge Arresters without Gaps for A.C. Systems. Geneva, Switzerland: IEC; 2014.
- [23] Ivanchenko AV, Tonkoshkur AS. Modeling of the degradation electromigrational processes in structures with intercrystallite potential barriers. *Multidiscipline Modeling in Materials and Structures* 2007; 3: 477-490.
- [24] Ivanchenko AV, Tonkoshkur AS. Electromigration degradation model of metal oxide varistor structures. *Ukrainian Journal of Physics* 2012; 57: 330.
- [25] Tonkoshkur AS, Glot AB, Ivanchenko AV. Percolation effects in dc degradation of ZnO varistors. *Journal of Advanced Dielectrics* 2015; 5: 1550008.
- [26] Cordaro JF, Shim Y, May JE. Bulk electron traps in zinc oxide varistors. *J Appl Phys* 1986; 60: 4186-4190.
- [27] Guo H, Liao H. Practical Approaches for Reliability Evaluation Using Degradation Data. In: 61st Annual Reliability and Maintainability Symposium; 26–29 January 2015; Palm Harbor, FL, USA.